Optical control of ground-state atomic orbital alignment: Cl($^2P_{3/2}$) atoms from HCl($v=2, J=1$) photodissociation

Dimitris Sofikitis
Institute of Electronic Structure and Laser, Foundation of Research and Technology-Hellas, 71110 Heraklion-Crete, Greece and Department of Physics, University of Crete, P.O. Box 2208, 71003 Voutes-Heraklion, Greece

Luis Rubio-Lago
Institute of Electronic Structure and Laser, Foundation of Research and Technology-Hellas, 71110 Heraklion-Crete, Greece

Marion R. Martin, Davida J. Ankeny Brown, and Nathaniel C.-M. Bartlett
Department of Chemistry, Stanford University, Stanford, California 94305-5080

Andrew J. Alexander
School of Chemistry, University of Edinburgh, West Mains Road, Edinburgh EH9 3JJ, United Kingdom

Richard N. Zare[a)]
Department of Chemistry, Stanford University, Stanford, California 94305-5080

T. Peter Rakitzis[b)]
Institute of Electronic Structure and Laser, Foundation of Research and Technology-Hellas, 71110 Heraklion-Crete, Greece and Department of Physics, University of Crete, P.O. Box 2208, 71003 Voutes-Heraklion, Greece

(Received 15 June 2007; accepted 23 July 2007; published online 10 October 2007)

$H^{35}Cl(v=0, J=0)$ molecules in a supersonic expansion were excited to the $H^{35}Cl(v=2, J=1, M=0)$ state with linearly polarized laser pulses at about 1.7 μm. These rotationally aligned $J=1$ molecules were then selectively photodissociated with a linearly polarized laser pulse at 220 nm after a time delay, and the velocity-dependent alignment of the $^{35}Cl(^2P_{3/2})$ photofragments was measured using 2+1 REMPI and time-of-flight mass spectrometry. The $^{35}Cl(^2P_{3/2})$ atoms are aligned by two mechanisms: (1) the time-dependent transfer of rotational polarization of the $H^{35}Cl(v=2, J=1, M=0)$ molecule to the $^{35}Cl(^2P_{3/2})$ nuclear spin [which is conserved during the photodissociation and thus contributes to the total $^{35}Cl(^2P_{3/2})$ photofragment atomic polarization] and (2) the alignment of the $^{35}Cl(^2P_{3/2})$ electronic polarization resulting from the photoexcitation and dissociation process. The total alignment of the $^{35}Cl(^2P_{3/2})$ photofragments from these two mechanisms was found to vary as a function of time delay between the excitation and the photolysis laser pulses, in agreement with theoretical predictions. We show that the alignment of the ground-state $^{35}Cl(^2P_{3/2})$ atoms, with respect to the photodissociation recoil direction, can be controlled optically. Potential applications include the study of alignment-dependent collision effects. © *2007 American Institute of Physics*. [DOI: 10.1063/1.2772272]

I. INTRODUCTION

Ground-state atomic orbital alignment plays an important role in chemical reactivity but has not been studied because of the difficulty in the preparation and control of aligned ground-state atoms. The reaction dynamics of orbitally aligned excited-state atoms has been studied in just a few cases, for atoms that can be excited conveniently with powerful visible lasers.[1–8] The Stern-Gerlach separation technique can produce polarized atomic beams, but the beam density is quite low, and to date no polarization-dependent reactive collision experiments have been reported using such polarized atomic beams (however, polarized atomic beams have been used extensively to study spin-dependent effects in nuclear and particle collisions).

Molecular photodissociation has been predicted to produce highly polarized atomic photofragments.[9–12] In recent years, such highly polarized atoms have been produced at high density in a few cases,[13–16] but particularly where the nuclear spin is 0 so that the electronic polarization is not depolarized by the nuclear spin.[17–21] In cases where the nuclear spin is not zero, the atomic orientation and alignment can be reduced significantly; for example, the degree of reduction in the alignment of ground-state Cl and Br atoms is about a factor of 4. Another potential drawback is that the degree of atomic alignment is fixed with respect to the recoil direction of the photofragments, so that if the recoil direction defines the reagent approach direction, as in photoloc

[a)]Electronic mail: zare@stanford.edu
[b)]Electronic mail: ptr@iesl.forth.gr

experiments,[22,23] then the atomic alignment cannot be controlled without further experimental modification. Such possible solutions include using magnetic fields to control the atomic polarization as desired or producing the photofragments from collimated molecular beams so that the atomic velocity can be controlled independently of the atomic polarization.

Recently, a new method was proposed to produce polarized photofragments from the photodissociation of rotationally state-prepared molecules that possess nonzero nuclear spins.[24,25] The parent molecules are excited to a rovibrational state with a polarized pulsed laser (the pump laser), with the goal of producing a high degree of alignment or orientation of the molecules in the excited state. The hyperfine states are not resolved, so that they are all excited coherently. The hyperfine beating that results from this coherent excitation produces a time-dependent polarization in the nuclear spins. When the polarization of the nuclear spins reaches a maximum (which in carefully selected cases can reach 100%), prompt photodissociation produces photofragments with highly polarized nuclear spins (which are either oriented or aligned, reflecting the initial polarization of the parent molecules' rotation). The production and control of the polarization of the nuclear spins of the photofragments allows us to address the two major disadvantages of the molecular photodissociation technique mentioned above (hyperfine depolarization and spatially fixed electronic polarization). The electronic angular momentum (J) polarization is fixed with respect to the photofragment recoil direction (and thus, on average, with respect to the photolysis laser polarization), whereas the nuclear spin angular momentum (I) polarization is fixed with respect to the pump laser polarization. The manner in which the two angular momenta are coupled can be controlled by the relative directions of the pump and photolysis polarizations and by the pump-photolysis time delay (since the nuclear polarization is time dependent). For example, at a certain pump-photolysis time delay the photofragment alignment can be large (where the alignments of J and I are of same sign and couple to give a large alignment), whereas at another delay the alignment can be negligible (where the alignments of J and I are of opposite sign and couple to give a small net alignment). This method was recently demonstrated for the production of oriented $Cl(^2P_{3/2})$ atoms from HCl photodissociation.[26]

The aim of this paper is to demonstrate the laser-based method described above for the production and control of *aligned* ground-state atoms, by applying it to the photodissociation of HCl molecules initially prepared in the ($v=2$, $J=1$, $M=0$) state, and by controlling the alignment (with respect to the recoil direction) of the resulting $Cl(^2P_{3/2})$ atomic photofragments. The control of the alignment of ground-state atoms will facilitate studies of the effects of electronic alignment in collision processes. The theory necessary to understand and analyze the measurements presented here is given in Sec. II, the experimental setup and procedures are described in Sec. III, and the results and discussion are given in Sec. IV.

II. THEORY

A. Time-dependent angular distributions of photofragment recoil

The spatial distribution of photofragments $I(\theta)$, in the axial recoil limit, from the photodissociation of molecules that have been prepared in the state $|JKM\rangle$, with respect to the axis of the linearly polarized photolysis light, is given by the product of spatial distribution of the bond alignment of the parent molecule $[d^J_{KM}(\theta)]^2$ with the angular distribution of the unpolarized molecules,[27,28] described by the well-known β parameter,[29]

$$I(\theta) = I_0[d^J_{KM}(\theta)]^2[1 + \beta P_2(\cos\theta)]. \tag{1}$$

For an ensemble of HCl($v=2, J=1$) molecules with M-state populations $p(J=1,M)$, the angular distribution is given by a population-weighted sum over M (note that $K=0$ for closed-shell diatomic molecules),

$$I(\theta) = I_0[1 + \beta P_2(\cos\theta)] \sum_{M=-1}^{M=+1} p(J=1,M)[d^1_{0M}(\theta)]^2. \tag{2}$$

The M-state distributions $p(J=1,M)$ of the HCl($v=2, J=1$) molecules, produced via a one-photon excitation from the HCl($v=0, J=0$) state using linearly polarized light, can be described in terms of a single molecule-alignment parameter, the $A_0^{(2)}(J,t)$,[24,30]

$$p(J=1, M=\pm 1) = \tfrac{1}{3}(1 + A_0^{(2)}(J,t)), \tag{3a}$$

$$p(J=1, M=0) = \tfrac{1}{3}(1 - 2A_0^{(2)}(J,t)). \tag{3b}$$

The time-dependent alignment $A_0^{(2)}(J_{HCl},t)$ can be expressed in terms of the alignment at $t=0$, the time of excitation of the HCl($v=2, J=1$) state, multiplied by the depolarization factor $G^{(2)}(t)$,[30]

$$A_0^{(2)}(J_{HCl},t) = G^{(2)}(t)A_0^{(2)}(J_{HCl}, t=0), \tag{4}$$

where $G^{(2)}(t)$ contains the time dependence of the alignment of J_{HCl}, arising from coupling to the Cl-atom nuclear spin via the hyperfine interaction and $A_0^{(2)}(J_{HCl}, t=0) = -1$, which, as shown by Eq. (3), describes the alignment of the initially prepared HCl($v=2, J=1, M=0$) state. The time dependence of $G^{(2)}(t)$ is expressed in terms of the energy splittings $(E_{F'} - E_F)$ between the hyperfine states with quantum number F, associated with the coupling $F = I_{Cl} + J_{HCl}$,[30]

$$G^{(2)}(t) = \sum_{F,F'} \frac{(2F'+1)(2F+1)}{(2I_{Cl}+1)} \begin{Bmatrix} F' & F & 2 \\ J_{HCl} & J_{HCl} & I_{Cl} \end{Bmatrix}^2 \times \cos((E_{F'} - E_F)t/\hbar). \tag{5}$$

As expected, $G^{(2)}(t=0) = 1$, i.e., there is no depolarization at $t=0$. Substituting Eqs. (3) and (4) into Eq. (2) and simplifying, we can express the photofragment angular distribution as

$$I(\theta) = \frac{I_0}{3}[1 + \beta P_2(\cos\theta)][1 + 2G^{(2)}(t)P_2(\cos\theta)]. \tag{6}$$

Finally, by multiplying out the product given in Eq. (6), the angular distribution can be expressed in terms of an expan-

sion of the first three even Legendre polynomials,

$$I(\theta) = I_0[1 + \beta_2 P_2(\cos\theta) + \beta_4 P_4(\cos\theta)], \tag{7}$$

where the coefficients β_2 and β_4 can be expressed in terms of the spatial anisotropy parameter β and $G^{(2)}(t)$ by

$$\beta_2 = \frac{\beta + 2G^{(2)}(t)(1 + (2/7)\beta)}{1 + (2/5)\beta G^{(2)}(t)} \tag{8a}$$

and

$$\beta_4 = \frac{(36/35)\beta G^{(2)}(t)}{1 + (2/5)\beta G^{(2)}(t)}. \tag{8b}$$

The spatial distribution of the photofragments from the photodissociation of the aligned HCl($v=2, J=1$) molecules, reported here, will be described using Eqs. (7) and (8), and the time-dependent term $G^{(2)}(t)$ will be described with Eq. (5).

B. Time-dependent photofragment angular momentum distributions

The alignment of the $^{35}Cl(^2P_{3/2})$ photofragments is produced from two mechanisms. First, the nuclear spin $I_{Cl}(t)$ is time-dependently aligned via polarization transfer from the molecular rotation of $H^{35}Cl(v=2, J=1, M=0)$; this polarization is conserved during the photodissociation step. Second, the photodissociation process itself aligns the electronic angular momentum $J_{Cl}(0)$ of the $^{35}Cl(^2P_{3/2})$ photofragments. Immediately after the production of the $^{35}Cl(^2P_{3/2})$ photofragments, the angular momenta $I_{Cl}(t)$ and $J_{Cl}(0)$ couple to give total angular momentum F. The resulting periodic polarization transfer between I_{Cl} and J_{Cl} occurs on the subnanosecond time scale, so that the experiments here (using laser pulses with durations of a few nanoseconds) are only sensitive to the time-averaged polarization $\langle J_{Cl}\rangle$, which is an average of the coupling of the initial polarizations of $I_{Cl}(t)$ and $J_{Cl}(0)$. In this section, we describe a simple model to calculate this time-averaged alignment.

The time dependence of the alignment of the nuclear spin $I_{Cl}(t)$ can be described by the alignment parameter $A_0^{(2)}(I_{Cl}, t)$, whose time dependence is described by the factor $H^{(2)}(I_{Cl}, t)$ multiplied by the original rotational polarization of the HCl parent molecule,[24,25]

$$A_0^{(2)}(I_{Cl}, t) = H^{(2)}(I_{Cl}, t) A_0^{(2)}(J_{HCl}, t = 0), \tag{9}$$

where

$$H^{(2)}(t) = \frac{U_2(I_{Cl})}{U_2(J_{HCl})} \sum_{F,F'} \frac{(2F'+1)(2F+1)}{\sqrt{(2I_{Cl}+1)(2J_{HCl}+1)}} (-1)^{(F-F')} \times \begin{Bmatrix} F' & F & 2 \\ J_{HCl} & J_{HCl} & I_{Cl} \end{Bmatrix} \begin{Bmatrix} F' & F & 2 \\ I_{Cl} & I_{Cl} & J_{HCl} \end{Bmatrix} \times \cos(E_{F'} - E_F)t/\hbar, \tag{10}$$

The polarization of the photofragment electronic angular momentum $J_{Cl}(0)$ with respect to the molecular frame of the photodissociation process is, in general, described by several polarization parameters, which are not measured in the current experiments.[10,31] We start off with the simplifying assumption that the alignment of $J_{Cl}(t=0)$ for all the photofragments, irrespective of their recoil direction, is described by a single laboratory-frame alignment parameter $A_0^{(2)}(J_{Cl}, t=0)$. This assumption allows us to calculate the time dependence of the $^{35}Cl(^2P_{3/2})$ photofragment alignment $A_0^{(2)}(J_{Cl}, t)$ and, by comparing to experiment, to infer the nascent photofragment electronic alignment $A_0^{(2)}(J_{Cl}, t=0)$. As shown in the results section, the fit to the data is sufficient so as not to justify further fit parameters, suggesting that the laboratory-frame nascent electronic alignment of the Cl-atom photofragments is satisfactorily described by the recoil-independent $A_0^{(2)}(J_{Cl}, t=0)$ parameter.

The calculation of the final time-averaged alignment of $\langle J_{Cl}\rangle$ from the initial alignment parameters $A_0^{(2)}(I_{Cl}, t)$ and $A_0^{(2)}(J_{Cl}, t=0)$ is carried out as follows. First, nuclear and electronic M-state populations $\rho_{M_{I_{Cl}} M_{I_{Cl}}}(t)$ and $\rho_{M_{J_{Cl}} M_{J_{Cl}}}$ are each calculated using the general formula (for $k=0$ and 2 only)[32]

$$\rho_{MM} = \sum_k \frac{(2k+1)[J(J+1)]^{k/2}}{c(k)\langle J\|J^{(k)}\|J\rangle} (-1)^{J-M} \begin{pmatrix} J & k & J \\ -M & 0 & M \end{pmatrix} \times A_0^{(k)}(J). \tag{11}$$

The M_F-state populations of the resulting total angular momentum F states, due to coupling $I_{Cl}(t)$ and $J_{Cl}(0)$, are calculated using the squares of Clebsch-Gordan coefficients for each pair of M states, weighting by the M-state populations $\rho_{M_{I_{Cl}} M_{I_{Cl}}}(t)$ and $\rho_{M_{J_{Cl}} M_{J_{Cl}}}$ and summing over all M states,

$$\rho_{M_F M_F}(F,t) = \sum_{M_{J_{Cl}}} \rho_{M_{J_{Cl}} M_{J_{Cl}}} \rho_{M_{I_{Cl}} M_{I_{Cl}}}(t) \times \langle J_{Cl} M_{J_{Cl}}, I_{Cl}(M_F - M_{J_{Cl}}) | F M_F\rangle^2 . \tag{12}$$

Note that the time dependence of $\rho_{M_F M_F}(F,t)$ is acquired from the time dependence of nuclear spin M-state distributions $\rho_{M_{I_{Cl}} M_{I_{Cl}}}(t)$. After decoupling, we calculate the final, time-averaged, M-state populations of $\langle J_{Cl}\rangle$ by summing over all possible ways that the states $|FM_F\rangle$ can decouple to give $|JM_{J_{Cl}}\rangle$ (the squares of the Clebsch-Gordan coefficients are weighted by the population of the M_F state, and we sum over all M_F states),

$$\langle \rho_{M_{J_{Cl}} M_{J_{Cl}}}(t)\rangle = \sum_{F, M_F} \rho_{M_F M_F}(F,t) \langle J_{Cl} M_{J_{Cl}}, I_{Cl} \times (M_F - M_{J_{Cl}}) | F M_F\rangle^2 . \tag{13}$$

Finally, the quadrupole moment of the time-averaged electronic alignment of the Cl atoms, the $A_0^{(2)}(J_{Cl}, t)$ parameter, can be calculated from the definition of the $A_0^{(2)}$ parameter, which is a weighted sum of the M-state populations,[30]

$$A_0^{(2)}(J_{Cl}, t) = \sum_{M_{J_{Cl}}} \langle \rho_{M_{J_{Cl}} M_{J_{Cl}}}(t)\rangle \left[\frac{3M_{J_{Cl}}^2}{J(J+1)} - 1 \right]. \tag{14}$$

III. EXPERIMENT

A 5% mixture of HCl in He was supersonically expanded into the extraction region of a Wiley-McLaren time-of-flight (TOF) mass spectrometer, described in detail

elsewhere,[22] via a pulsed nozzle operating at 20 Hz, using a backing pressure that ranged between 0.5 and 1 bar, which cooled the HCl to a rotational temperature of about 15 K. The predominately populated $H^{35}Cl(v=0,J=0)$ state is subsequently excited to the $H^{35}Cl(v=2,J=1,M=0)$ state with linearly polarized infrared (IR) light. The IR light was generated by difference frequency mixing the fundamental of an injection-seeded Nd^{3+}: yttrium aluminum garnet (YAG) laser (Continuum, PL9020) with the ~664 nm output of a dye laser (Continuum, ND6000, Exciton: DCM) to make light around 1.767 μm.[33] This light is amplified in an optical parametric amplification stage to produce ~30 mJ of linearly polarized tunable radiation with a bandwidth of ~1.0 cm^{-1}. The splitting between $F_1=1/2$ and $F_1=3/2$ lines in the $J=1-0$ microwave spectrum of $H^{35}Cl$ is 30.4 MHz.[34] The coherence width of the IR pump pulse is ~100 MHz, meaning that all the hyperfine states are coherently excited. The $H^{35}Cl(v=2,J=1)$ molecules were photodissociated after a variable time delay with a linearly polarized laser pulse at 220 nm, and the $^{35}Cl(^2P_{3/2})$ atomic photofragments were ionized by 2+1 REMPI via the $4p\ ^2P_{1/2} \leftarrow 3p\ ^2P_{3/2}$ two-photon transition, using linearly polarized light at 234.63 nm,[35] timed to be immediately after the photolysis laser pulse. The UV light for the REMPI step is generated by frequency doubling in a beta barium borate (BBO) crystal the output of a Nd:YAG-pumped dye laser (Exciton, Coumarin 480), using about 0.1 mJ/pulse. The 220 nm light for photolysis is generated by frequency tripling in two BBO crystals the output of a separate Nd:YAG-pumped dye laser (Exciton, DCM), using about 1.0 mJ/pulse. All three lasers had pulse widths of a few nanoseconds. The direction of the linear polarization of the probe light was alternated between horizontal and vertical on a shot-to-shot basis using a photoelastic modulator (PEM 80 Hinds Electronics) to produce ionization signals with the probe polarization parallel and perpendicular to the TOF axis, denoted by $I(\parallel)$ and $I(\perp)$, respectively. The $^{35}Cl^+$ ions were detected with the TOF mass spectrometer for delays of 0–200 ns between the pump (IR) laser pulse and the photolysis and probe (UV) laser pulses.

IV. RESULTS AND DISCUSSION

Figure 1 shows a typical isotropic-sum time-of-flight profile of the ionized $Cl(^2P_{3/2})$ photofragments from the photodissociation of the $HCl(v=2,J=1)$ state. The isotropic-sum profile is given by adding $I(\parallel)+2I(\perp)$, where $I(\parallel)$ and $I(\perp)$ are the signals produced with the probe linear polarization parallel or perpendicular to the TOF axis, respectively. Such a sum is insensitive to any $k=2$ angular momentum alignment parameters,[23] for an experimental geometry which otherwise is cylindrically symmetric about the TOF axis, as in this case (the pump and photolysis lasers are linearly polarized parallel to the TOF axis). The alignment of the $Cl(^2P_{3/2})$ photofragments is described by even k polarization parameters, where $k \leqslant 2J$. As $J_{Cl}=3/2$, the only allowed nonzero parameters are for $k=2$, such as $A_0^{(2)}(J_{Cl},t)$.

The shape of the isotropic-sum profile is, therefore, only

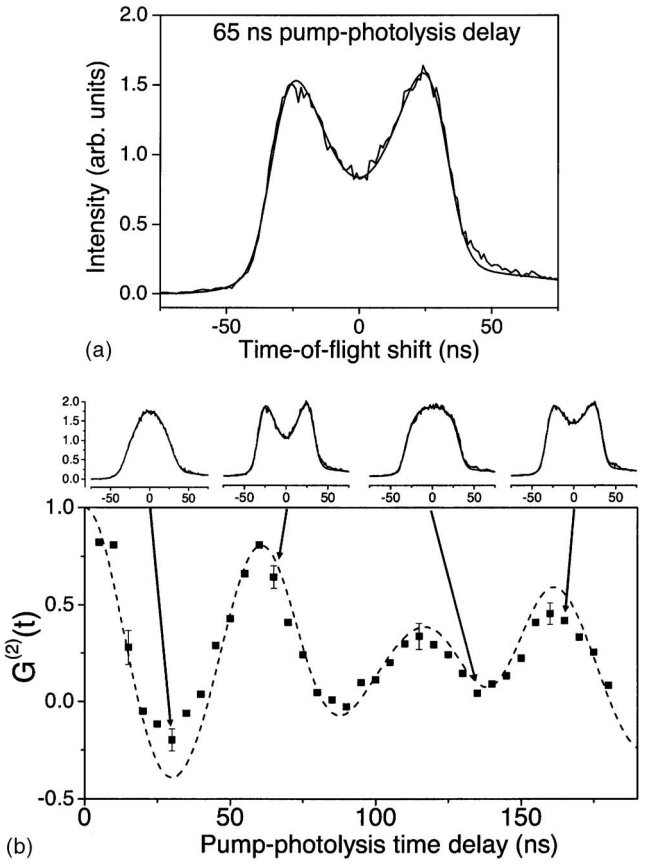

FIG. 1. (a) Isotropic-sum profile $I(\parallel)+2I(\perp)$ for $^{35}Cl(^2P_{3/2})$ photofragments at a pump-photolysis delay of 65 ns. This sum profile is not sensitive to the photofragment angular momentum alignment, and it contains information only about the photofragment recoil spatial distribution. The profile is fitted for the spatial anisotropy β parameter, as well as the degree of parent molecule bond alignment as a function of the $G^{(2)}(t)$ parameter (see text for details). (b) Isotropic-sum profiles, as in (a), are analyzed for the value of $G^{(2)}(t)$ for pump-photolysis delays between 0 and 200 ns. The shapes of the profiles are shown to vary considerably with the time delay (upper inset), and the measured values of $G^{(2)}(t)$ (solid squares) agree well with theory (dashed line).

sensitive to the spatial anisotropy of the photofragment velocities, as described by Eqs. (7) and (8). For the prompt photodissociation of HCl, the Cl recoil direction is very closely parallel to the HCl bond; therefore, the measurement of the angular distribution of the Cl recoil directions gives information on the degree of alignment of the HCl bond axis in space. This hyperfine beating of the spatial distribution of the angular momentum of aligned HCl molecules has been measured,[36,37] and it has been well described by the depolarization coefficient $G^{(2)}(t)$ [see Eq. (5)]. The bond axis of HCl is always perpendicular to the rotational angular momentum; therefore, the spatial distribution of the HCl bond in space should show the same hyperfine beating effect that has been measured for the rotational angular momentum.

The upper inset of Fig. 1(b) shows that the TOF profiles change significantly in shape as a function of the time delay between the pump and the photolysis/probe lasers, showing that the bond alignment of the $HCl(v=2,J=1)$ state is changing in time, as described in Sec. II A. The profiles are fitted to the function

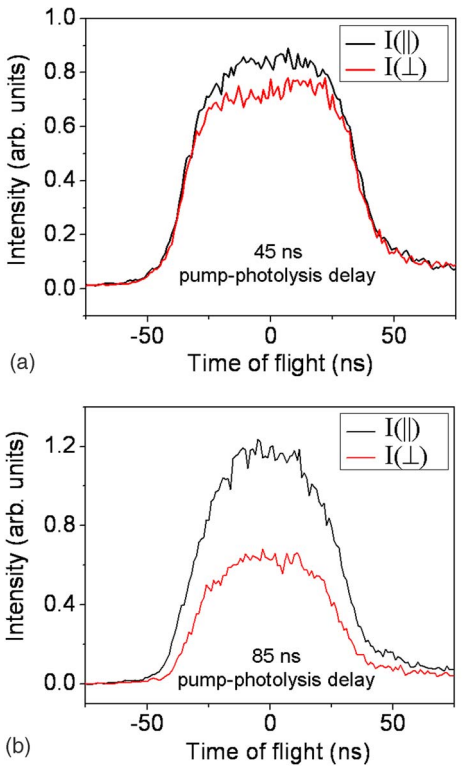

FIG. 2. (Color online) Pairs of time-of-flight profiles of $^{35}Cl(^2P_{3/2})$ photofragments with the probe laser parallel, $I(\parallel)$ (upper line), and perpendicular $I(\perp)$ (lower line), to the TOF axis, for pump-photolysis delays of (a) 45 ns and (b) 85 ns. The difference in the $I(\parallel)$ and $I(\perp)$ profiles is small for (a), whereas it is considerably larger for (b), showing that the alignment of the ground-state $^{35}Cl(^2P_{3/2})$ atoms can be controlled optically.

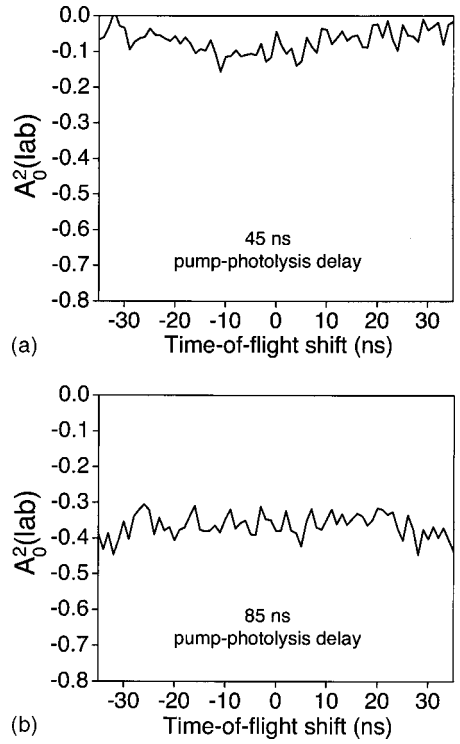

FIG. 3. The spatial dependences of the laboratory-frame alignment $A_0^{(2)}(J_{Cl},t)$ of the profiles shown in Fig. 3 are calculated using Eq. (16) applied to the $I(\parallel)$ and $I(\perp)$ profiles. In both cases, the alignment is approximately constant over the whole profile. For the photofragments with recoils parallel to the TOF axis, we see that for (a) at a pump-photolysis delay of 45 ns, $A_0^{(2)}(J_{Cl},t)\approx -0.05$, whereas for (b) at a pump-photolysis delay of 85 ns, $A_0^{(2)}(J_{Cl},t)\approx -0.4$ [the physical range of $A_0^{(2)}(J_{Cl},t)$, for $J=3/2$, is from −0.8 to +0.8].

$$I(x_D) = I_0[1 + \beta_2 P_2(x_D) + \beta_4 P_4(x_D)], \tag{15}$$

where x_D is the normalized shift along the TOF axis ($x_D = v_{TOF}/|\mathbf{v}|$), and ranges from −1 to +1. The coefficients β_2 and β_4, as shown in Eq. (8), are expressed in terms of the spatial anisotropy parameter β and by the depolarization coefficient $G^{(2)}(t)$. For each profile, the β parameter is the same, whereas all of the time dependence is expressed in $G^{(2)}(t)$. Fitting the profiles yields $\beta = -0.3 \pm 0.2$, whereas the time dependence of $G^{(2)}(t)$ is shown in Fig. 1(b), and agreement with theory is good.

Pairs of profiles $I(\parallel)$ and $I(\perp)$ with the probe polarization parallel and perpendicular to the TOF axis, respectively, are shown in Fig. 2. One pair is measured at a pump-photolysis delay of (a) 45 ns, where the difference between $I(\parallel)$ and $I(\perp)$ is small [thus $A_0^{(2)}(J_{Cl},t)$ is small], and the other pair at a delay of (b) 85 ns, where the difference between $I(\parallel)$ and $I(\perp)$ is large [thus $A_0^{(2)}(J_{Cl},t)$ is large].

Information about the alignment of the $Cl(^2P_{3/2})$ photofragments is given by differences in the profiles $I(\parallel)$ and $I(\perp)$. In particular, the laboratory-frame alignment parameter $A_0^{(2)}(J_{Cl},t)$ is given by

$$A_0^{(2)}(J_{Cl},t) = \frac{2}{s_2}\frac{[I(\parallel) - I(\perp)]}{[I(\parallel) + 2I(\perp)]}, \tag{16}$$

where s_2 is the experimental sensitivity to the alignment parameter; for the REMPI scheme used here (see Sec. III), $s_2 = -5/4$. The value of $A_0^{(2)}(J_{Cl},t)$ can be determined as a function of Doppler shift across the profile, and these values are shown in Fig. 3, for the pump-photolysis time delays of (a) 45 ns and (b) 85 ns. In both cases, the value of the $A_0^{(2)}(J_{Cl},t)$ parameter does not change strongly over the profile. For the photofragments recoiling parallel to the TOF axis, the alignment is approximately $A_0^{(2)}(J_{Cl},t)\approx -0.05$ for case (a) and $A_0^{(2)}(J_{Cl},t)\approx -0.4$ for case (b), for these particular data sets.

$A_0^{(2)}(J_{Cl},t)$ can vary, as a function of the Dopper shift x_D, as an even expansion of Legendre polynomials terminated at the fourth order,

$$A_0^{(2)}(J_{Cl},t,x_D) = c_0 + c_2 P_2(x_D) + c_4 P_4(x_D). \tag{17}$$

The coefficients c_k can be expressed in terms of the molecular frame polarization parameters, using Eq. (4) of Ref. 38, by setting $\Gamma = 0$, and finding the coefficients of $P_2(\cos\Delta)$ (notice that $\cos\gamma$ is equivalent to x_D),

$$c_0 = \tfrac{2}{15}[(1+\beta)a_0^2(\parallel) - (1-\beta/2)a_0^2(\perp) + \sqrt{6}a_1^2(\parallel,\perp) + 2\sqrt{6}(1-\beta/2)a_2^2(\perp)], \tag{18a}$$

$$c_2 = \tfrac{1}{21}[11(1+\beta)a_0^2(\parallel) + 10(1-\beta/2)a_0^2(\perp) + 2\sqrt{6}a_1^2(\parallel,\perp) - 8\sqrt{6}(1-\beta/2)a_2^2(\perp)], \tag{18b}$$

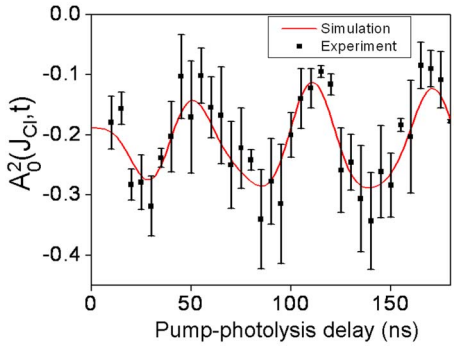

FIG. 4. (Color online) The average value of the photofragment alignment (integrated over all recoil directions) as a function of pump-photolysis delay. The general shape of the time dependence of the experimental points (solid squares) is described well by the model calculations (solid line) as detailed in the text.

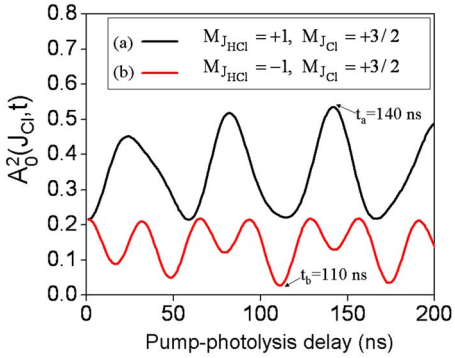

FIG. 5. (Color online) The Cl-atom alignment is calculated for the (hypothetical) case of the photodissociation of HCl yielding photofragments with electronic angular momentum described by $J_{Cl}=3/2$, $M_{Cl}=3/2$, after it has coupled with the nuclear spin alignment, which was produced from the polarization transfer from HCl rotation in (a) the state $J_{HCl}=1$, $M_{HCl}=+1$ (black, upper line) and (b) $J_{HCl}=1$, $M_{HCl}=-1$ (red, lower line). This simulation shows that for this favorable case, the $Cl(^2P_{3/2})$ atom alignment can be controlled to vary between the large value of $A_0^{(2)}(J_{Cl},t)\approx 0.54$ for a pump-photolysis delay of (a) $t_a=140$ ns and can be reduced to nearly 0 at a pump-photolysis delay of (b) $t_b=110$ ns.

$$c_4=\tfrac{4}{35}[3(1+\beta)a_0^2(\|)-3(1-\beta/2)a_0^2(\perp)-2\sqrt{6}a_1^2(\|,\perp)+\sqrt{6}(1-\beta/2)a_2^2(\perp)]. \quad (18c)$$

The model used here assumes that c_2 and c_4 are zero, which is justified by the observation that the alignment does not change strongly over the profile. For each of the profiles with time delays from 0 to 200 ns, an average value of $A_0^{(2)}(J_{Cl},t)$ was determined by integrating the profiles $I(\|)$ and $I(\perp)$ and inserting these integrated values in Eq. (16). The results are given in Fig. 4, along with the calculated model of the results, as described by Eq. (14) (see Sec. II B for details). For the model, the initial value of the electronic alignment of the $Cl(^2P_{3/2})$ atoms in the lab frame, produced by the photodissociation step, is nearly maximal: $A_0^{(2)}(J_{Cl},t=0)=-0.7$. This value, along with the near zero values of the c_2 and c_4 coefficients in Eq. (17), is not consistent with the values of the polarization parameters measured and calculated from the photodissociation of HCl at 193 nm,[14–16,39] indicating that the vibrational excitation of HCl changes the dynamics of the photodissociation (shown also by the beta parameter value of about −0.3, compared to close to −1 at 193 nm). The model fits the general trends of the data in Fig. 4 fairly well, but the amplitude of the modulations seems to be somewhat smaller than the data. We believe that the simplifications of the model (necessitated by the lack of knowledge of the complete density matrix of the photofragments) are responsible for any small discrepancies.

We have shown the ability to vary the alignment of the ground-state $Cl(^2P_{3/2})$ atoms, using this optical technique, from about $A_0^{(2)}(J_{Cl},t)\approx -0.05$ to $A_0^{(2)}(J_{Cl},t)\approx -0.4$. This variation, from about zero alignment to half the physical maximum, is large enough to study the effect of the electronic alignment in collision processes that have experimental signal-to-noise ratios of a few percent. The modulation of the alignment, in this case, is somewhat limited by the initial negative alignment of the Cl photofragments $[A_0^{(2)}(J_{Cl},t=0)=-0.7$, as found from the modeling]. If the alignment were instead large and positive $[A_0^{(2)}(J_{Cl},t=0)=+0.8]$, then we show that a larger alignment modulation could be produced. In this hypothetical case, the pump laser pulse is flipped between left and right circularly polarized states, which allows the HCl molecules to be prepared in either the $HCl(v=2,J=1,M=+1)$ or $HCl(v=2,J=1,M=-1)$ states.[40] The photolysis laser is then left circularly polarized (with respect to the IR laser) so that the nascent $Cl(^2P_{3/2})$ photofragments recoiling along the laser propagation direction would populate the ($J_{Cl}=3/2$, $M_{Cl}=+3/2$) state. Coupling the polarized Cl-atom nuclear spin (which is polarized by transfer from the HCl rotational polarization) to the polarized $Cl(^2P_{3/2})$ electronic angular momentum J_{Cl} yields the final alignment $A_0^{(2)}(J_{Cl},t)$ of the $Cl(^2P_{3/2})$ atoms, which is shown in Fig. 5. The modulation of the alignment in this case is shown to vary from as high as about 0.54 (for parallel helicities of the pump and photolysis laser, at a delay of 140 ns), to as low as about 0.03 (for antiparallel helicities of the pump and photolysis laser, at a delay of 110 ns).

ACKNOWLEDGMENTS

We gratefully acknowledge support from the G.S.R.T. Bilateral Collaboration grant Greece-U.S.A. (05NON-EU-68), the European Commission transfer of knowledge grant SOUTHERN DYNAMICS MTKD-CT-2004-014306, and the U.S. National Science Foundation Grant No. 0242103. One of us (M.R.M.) thanks the National Football Foundation and College Hall of Fame for a scholar-athlete award.

[1] C. T. Rettner and R. N. Zare, J. Chem. Phys. **77**, 2416 (1982).
[2] A. G. Suits, H. Hou, H. F. Davis, Y. T. Lee, and J. M. Mestdagh, J. Chem. Phys. **95**, 8178 (1991).
[3] A. G. Suits, H. Hou, H. F. Davis, and Y. T. Lee, J. Chem. Phys. **96**, 2777 (1992).
[4] K. C. Lin, P. D. Kleiber, J. X. Wang, W. C. Stwalley, and S. R. Leone, J. Chem. Phys. **89**, 4771 (1988).
[5] C. J. Smith, J. P. J. Driessen, L. Eno, and S. R. Leone, J. Chem. Phys. **96**, 8212 (1992).
[6] C. J. Smith, E. M. Spain, M. J. Dalberth, S. R. Leone, and J. P. J. Driessen, J. Chem. Soc., Faraday Trans. **89**, 1401 (1993).
[7] E. M. Spain, M. J. Dalberth, P. D. Kleiber, S. R. Leone, S. S. Op de Beek, and J. P. J. Driessen, J. Chem. Phys. **102**, 9532 (1995).
[8] G. Ding, W. Sun, W. Yang, D. Xu, R. Zhao, G. He, and N. Lou, Chem. Phys. Lett. **265**, 392 (1997).

[9] R. J. van Brunt and R. N. Zare, J. Chem. Phys. **48**, 4304 (1968).
[10] L. D. A. Siebbeles, M. Glass-Maujean, O. S. Vasyutinskii, J. A. Beswick, and O. Roncero, J. Chem. Phys. **100**, 3610 (1994).
[11] G. G. Balint-Kurti, A. J. Orr-Ewing, J. A. Beswick, A. Brown, and O. S. Vasyutinskii, J. Chem. Phys. **116**, 10760 (2002).
[12] A. J. Alexander and R. N. Zare, Acc. Chem. Res. **33**, 199 (2000).
[13] A. S. Bracker, E. R. Wouters, A. G. Suits, and O. S. Vasyutinskii, J. Chem. Phys. **110**, 6749 (1999).
[14] T. P. Rakitzis, P. C. Samartzis, R. L. Toomes, L. Tsigaridas, M. Coriou, D. Chestakov, A. T. J. B. Eppink, D. H. Parker, and T. N. Kitsopoulos, Chem. Phys. Lett. **364**, 115 (2002).
[15] T. P. Rakitzis, P. C. Samartzis, R. L. Toomes, T. N. Kitsopoulos, A. Brown, G. G. Balint-Kurti, O. S. Vasyutinskii, and J. A. Beswick, Science **300**, 1936 (2003).
[16] T. P. Rakitzis, P. C. Samartzis, R. L. Toomes, and T. N. Kitsopoulos, J. Chem. Phys. **121**, 7222 (2004).
[17] A. T. J. B. Eppink, D. H. Parker, M. H. M. Janssen, B. Buijsse, and W. J. van der Zande, J. Chem. Phys. **108**, 1305 (1998).
[18] M. Ahmed, D. S. Peterka, A. S. Bracker, O. S. Vasyutinskii, and A. G. Suits, J. Chem. Phys. **110**, 4115 (1999).
[19] Y. Mo, H. Katayanagi, M. C. Heaven, and T. Suzuki, Phys. Rev. Lett. **77**, 830 (1996).
[20] T. P. Rakitzis, P. C. Samartzis, and T. N. Kitsopoulos, Phys. Rev. Lett. **87**, 123001 (2001).
[21] D. Townsend, S. K. Lee, and A. G. Suits, Chem. Phys. **301**, 197 (2004).
[22] W. R. Simpson,A. J. Orr-Ewing, T. P. Rakitzis, S. A. Kandel, and R. N. Zare, J. Chem. Phys. **103**, 7313 (1995).
[23] T. P. Rakitzis, S. A. Kandel, and R. N. Zare, J. Chem. Phys. **107**, 9382 (1997).
[24] T. P. Rakitzis, Phys. Rev. Lett. **94**, 083005 (2005).
[25] L. Rubio-Lago, D. Sofikitis, A. Koubenakis, and T. P. Rakitzis, Phys. Rev. A **74**, 042503 (2006).
[26] D. Sofikitis, L. Rubio-Lago, M. R. Martin, D. J. A. Brown, N. C.-M. Bartlett, R. N. Zare, and T. P. Rakitzis, Phys. Rev. A **76**, 012503 (2007).
[27] S. E. Choi and R. B. Bernstein, J. Chem. Phys. **85**, 150 (1986).
[28] R. N. Zare, Chem. Phys. Lett. **156**, 1 (1989).
[29] R. N. Zare, Mol. Photochem. **4**, 1 (1972).
[30] R. N. Zare, *Angular Momentum* (Wiley, New York, 1988).
[31] T. P. Rakitzis and R. N. Zare, J. Chem. Phys. **110**, 3341 (1999).
[32] A. J. Orr-Ewing and R. N. Zare, Annu. Rev. Phys. Chem. **45**, 315 (1994).
[33] J. P. Camden, H. A. Bechtel, D. J. Ankeny Brown, A. E. Pomerantz, R. N. Zare, and R. J. Le Roy, J. Phys. Chem. A **108**, 7806 (2004).
[34] F. C. De Lucia, P. Helminger, and W. Gordy, Phys. Rev. A **3**, 1849 (1971).
[35] NIST, 2006. Atomic spectra database, http://physics.nist.gov/PhysRefData/ASD/index.html
[36] A. J. Orr-Ewing, W. R. Simpson, T. P. Rakitzis, and R. N. Zare, Isr. J. Chem. **34**, 95 (1994).
[37] H. Lammer, R. T. Carter, and J. R. Huber, Eur. Phys. J. D **8**, 385 (2000).
[38] T. P. Rakitzis, G. E. Hall, M. Costen, and R. N. Zare, J. Chem. Phys. **111**, 8751 (1999).
[39] A. Brown, G. G. Balint-Kurti, and O. S. Vasyutinskii, J. Phys. Chem. A **108**, 7790 (2004).
[40] A. J. Alexander, J. Chem. Phys. **123**, 194312 (2005).